Pharmacogn. Commn. 2019; 9(3): 85-90
A multifaceted peer reviewed journal in the field of Pharmacognosy and Natural Products
www.phcogcommn.org

Original Article

Inhalation Absorption Prediction (IAP) Model for Predicting Medicinal Cannabis Phytochemical Pharmacokinetics

Kimber Wise[1,2], Harsharn Gill[1], Jamie Selby-Pham[2,*]
[1]School of Science, RMIT University, Bundoora VIC 3083, AUSTRALIA.
[2]Nutrifield, Sunshine West VIC 3020, AUSTRALIA.

ABSTRACT

Introduction: The medicinal benefits from inhalation of *Cannabis sativa* phytochemicals have been extensively reported. Whilst *in-silico* models are available for prediction of phytochemical pharmacokinetics post-ingestion, no models are available to accurately predict inhalation pharmacokinetics. Therefore, the aim of this study was to explore the relationship between phytochemical physicochemical properties and inhalation pharmacokinetics and to develop an *in-silico* model for predicting the time of maximal compound concentration in plasma (T_{max}) and compound elimination half-life ($T_{½}$), following inhalation. **Methods:** A training set of compound pharmacokinetic data was collated from previous publications and compared to physicochemical parameters using regression analyses. Physicochemical parameters that correlated with T_{max} and $T_{½}$ were combined to develop a statistical model, which constructs functional fingerprints predicting compound concentrations in plasma post inhalation. Predicted functional fingerprints for three cannabis bioactive compounds were constructed and biomatched against previously reported physiological effects. **Results:** Inhalation T_{max} was predicted (r^2 = 0.84) by compound volume (Vol), topological surface area (TPSA) and molecular weight (MW), whilst $T_{½}$ was predicted (r^2 = 0.87) by molecular weight, volume and number of rotatable bonds (nrot). The resulting inhalation absorption prediction (IAP) model was achieved by combining T_{max} and $T_{½}$ predictions. The IAP model was applied to cannabis metabolites which accurately predicted decay functions *in-vivo* and biomatching with associated physiological effects. **Conclusion:** The IAP model was applied successfully to cannabis phytochemicals to explore the pharmacokinetics underpinning their medicinal effects. This study demonstrates the utility of the IAP model and highlights its applicability during the investigation of medicinal plants and their modes of action.

Key words: Biomatching, Pharmacognosy, Functional fingerprint, Medicinal plants.

Correspondence:
Dr. Jamie Selby-Pham
Head of R&D/ Chief Research Scientist, Nutrifield, Sunshine West, VIC-3020, AUSTRALIA.
Phone no: +61 (3) 9315 5815
E-mail: Jamies@nutrifield.com.au
DOI: 10.5530/pc.2019.3.18

INTRODUCTION

In many cultures, *Cannabis sativa* (cannabis) has been a traditionally valuable crop, heralded for its versatility as a fibre, food source, recreational drug and medicine.[1] It's use in ethnopharmacology is well established for treatment of pain and inflammation[2] and it is now the target of pharmacognosy studies to explore the potential of application within conventional medicine for treatment of ailments including cancer, pain, loss of appetite, nausea, vomiting, anxiety and drug resistant epilepsy.[3,4] Traditionally the cannabis plant is smoked or consumed orally as a tea or in foods[5] and smoking remains the most popular intake method today.[6] Although medicinal efficacy of cannabis is largely attributed to the presence of cannabinoids, in particular the psychoactive cannabinoid delta-9-tetrathydrocannabinol (THC), cannabis plant material contains many other bioactive compounds which may also be contributing to its therapeutic effect.[2,7,8] Plant extracts containing multiple bioactive compounds have been shown to exhibit enhanced medicinal efficacy than the sum of their individual components, a phenomenon known as pharmacodynamic synergy or the entourage effect.[9,10] Accordingly, cannabinoid and non-cannabinoid phytochemicals may be individually or synergistically contributing to the medicinal efficacy of cannabis.

Understanding the pharmacokinetics of medicinal compounds is critical for establishing safe and effective administration practises. While *in-vivo* approaches may be preferred, *in-silico* predictive models have proven to be powerful, cost-effective tools, for fast and efficient pharmacokinetic approximations to guide usage and designing future clinical studies.[11] The *in-silico* phytochemical absorption prediction (PCAP) model presented in Selby-Pham *et al.*[12] has been applied to predict phytochemical pharmacokinetics of plant extracts to guide recommended intake times for maximal health benefits.[13] This optimisation utilises the concept of 'biomatching', wherein maximal medicinal efficacy is achieved by aligning plasma concentrations of stress-mediating compounds with periods of associated stressors.[12,14] For example, extracts from *Hyptis sp.* and *Hypericum perforatum* were recommended to be ingested two hours prior to meals to achieve maximal stress mediation from absorbed antioxidant phytochemicals by biomatching the time of maximal plasma concentration (T_{max}) with the period of postprandial oxidative stress.[15,16] Accordingly, the capacity to predict T_{max} has allowed determination of optimal intake times to biomatch chemical activities with the timings of their maximal benefit.

Elimination half-life ($T_{½}$) describes time for plasma drug concentrations (PDC) to halve following intake and thereby guides determination of loading dosages, dosing intervals and bolus dose.[17,18] Accordingly, the $T_{½}$ of medicinal compounds must be accounted for when determining dosage regimens to ensure that PDC remains within the effective range and does not reach toxic or subtherapeutic levels.[19] Whilst the PCAP model is available for *in-silico* pharmacokinetic predictions following ingestion, no equivalent model for predicting inhalation pharmacokinetics is well established. The PCAP model targets intake time to maximise health benefits of ingested compounds by biomatching T_{max} with peak time of stressors. By contrast, health benefits of inhaled compounds are maximised by targeting dosing intervals to maintain effective PDC range based on $T_{½}$, as T_{max} for inhaled compounds is near instant and provides little room for optimisation.[20] Herein the *in-silico* inhalation absorption prediction (IAP) model is presented for predicting the pharmacokinetics (T_{max} and $T_{½}$) of phytochemicals and other compounds following inhalation. The model is used to develop functional fingerprints for bioactive phytochemicals, which can be used to achieve biomatching of their maximal activity with optimal effect time.

MATERIALS AND METHODS

Inhalation Absorption Prediction (IAP) model development

A training set of *in-vivo* pharmacokinetic data from 14 inhaled compounds (isolated compounds or compounds present within their native plant-material matrix) was used to develop regression equations for T_{max} and $T_{½}$. *In-vivo* pharmacokinetic data was sourced from the following publications: Cass *et al.*,[21] Cone,[22] Drollmann *et al.*,[23] Jäger *et al.*,[24] Kirby *et al.*,[25] Lecaillon *et al.*,[26] Marsot *et al.*,[27] Neale *et al.*,[28] Richards *et al.*,[29] Rix *et al.*,[30] Schneider *et al.*,[31] Skoner[32] Spyker *et al.*,[33] Thorsson *et al.*,[34] Usmani *et al.*,[35] and Vaisman *et al.*[36] Physicochemical data for training compounds was collected from the online property calculation toolkit, Molinspiration (http://www.molinspiration.com). Physicochemical measures utilised included molecular weight (MW), lipophilicity descriptor (log P), topological polar surface area (TPSA), number of freely rotatable bonds (nrot) and molecular volume (Vol). The relationship between the physicochemical data and the published T_{max} and $T_{½}$ was explored by statistical analyses to identify physicochemical properties with predictive power for each pharmacokinetic measure. Linear regressions were performed in Minitab 18 statistical software (Minitab Inc., State College, Pennsylvania, USA). The equations predicting T_{max} and $T_{½}$ from physicochemical properties and their application to produce functional fingerprints for plasma concentration following inhalation, are herein referred to as the inhalation absorption prediction (IAP) model.

Production of functional fingerprints

Functional fingerprints were generated as per the IAP model using predicted T_{max} and $T_{½}$ for test compounds (equations 1 and 2). In short, equations 1 and 2 were used to calculate 7 key pharmacokinetic time points (T_1=T_0, T_2=T_{max}, T_3=$T_{½}$, T_4=2*$T_{½}$, T_5=3*$T_{½}$, T_6=4*$T_{½}$ and T_7=5*$T_{½}$), with the plasma concentration at T_1 assigned a value of 0 and T_2 (T_{max}) assigned the maximal plasma concentration (C_{max}) if known, else a relative value of 100%. Additionally, T_3 ($T_{½}$) through T_7, representing 5 half-lives, were assigned plasma concentrations half that of their previous time point. These time points were connected via 6 regression equations ($y=m_1x+c_1$, $y=m_2x+c_2$, $y=m_3x+c_3$, $y=m_4x+c_4$, $y=m_5x+c_5$ and $y=m_6x+c_6$) to produce a functional fingerprint describing predicted plasma concentration over time following inhalation at T_1.

Biomatching of cannabis phytochemicals

The IAP model was applied to data from Mediavilla and Steinemann[37] and Greenwald and Stitzer[38] to produce functional fingerprints for three cannabis phytochemicals; THC, myrcene and caryophyllene. The functional fingerprints were compared to data from Greenwald and Stitzer[38] to explore temporal biomatching between plasma concentrations of the three phytochemicals and observed physiological effects, following inhalation of cannabis treatment or placebo cigarettes. In short, the study by Greenwald and Stitzer[38] involved patients smoking 4 bouts of 3 cigarettes weighing between 750 to 990 mg followed by testing for a range of physiological and psychological effects. Cannabis THC concentrations were determined from Greenwald and Stitzer[38] whilst myrcene and caryophyllene concentrations were based on the medicinal strain "Swiss mix" and fibre strain "Fedora" from Mediavilla and Steinemann,[37] as representative profiles of the treatment and placebo cigarettes, respectively. The treatment cigarettes (49.3% myrcene, 19.5% caryophyllene and 3% THC) were inhaled in combination with placebo cigarettes (29.4% myrcene, 37.5% caryophyllene and 0% THC) in Greenwald and Stitzer[38] to achieve overall phytochemical inhalation described in Table 1.

Table 1: Amount of compound inhaled following cannabis treatment and placebo cigarettes.

Compound	Mass of compound inhaled (mg)			
	Bout 1	Bout 2	Bout 3	Bout 4
THC	0	31	62	93
Myrcene	767	940	1114	1287
Caryophyllene	979	822	666	509

RESULTS AND DISCUSSION

Development of the Model

The IAP model was developed using a training data set of 14 medicinal compounds administered by inhalation, with T_{max} and $T_{½}$ identified in previous studies. The range of T_{max} and $T_{½}$ values were 0.02–1.00 h and 1.74–18.75 h, respectively and the range of physicochemical measures were as follows: molecular weight (MW) 154.25–538.58 g/mol, lipophilicity descriptor (log P) -3.64–6.69, topological polar surface area (TPSA) 9.23–200.72, number of freely rotatable bonds (nrot) 0–8 and molecular volume (Vol) 165.62–451 Å^3.

Preliminary model development explored the relationships between individual physicochemical parameters and the pharmacokinetic measures T_{max} and $T_{½}$. Individual physicochemical parameters had poor predictive power (Supplemental Table S3), with visualisation of either T_{max} or $T_{½}$ with singular physicochemical measures (Figure 1) suggesting the possibility for non-linear relationships or the necessity for multiple measures to achieve predictive power. This is consistent with previous pharmacokinetic studies, such as the PCAP model,[12] which have shown that following consumption, individual measures had poor predictive power while a combination of measures could be used to achieve a model with greater predictive power.

Pearson's correlation coefficients (Supplement Table S2) were used to assess the power of physicochemical properties to predict pharmacokinetic properties based on the categorisation of strength of correlation as; $r < 0.3$ negligible, $0.3 < r < 0.5$ low, $0.5 < r < 0.7$ moderate, $0.7 < r < 0.9$ high and $r > 0.9$ very high.[39] T_{max} showed negligible correlation with nrot ($r = 0.171$), low correlation with log P (r = 0.343), Vol ($r = 0.403$) and MW ($r = 0.412$) and a moderate correlation with TPSA ($r = 0.576$). By contrast, $T_{½}$ showed a negligible correlation with TPSA ($r = 0.010$), low correlation with nrot ($r = 0.329$) and log P ($r = 0.349$) and a moderate correlation with Vol ($r = 0.506$) and MW ($r = 0.528$). These results were dissimilar to Selby-Pham *et al.*[12] which observed moderate correlation for molecular weight and high correlation for log P and TPSA to T_{max} following ingestion. Accordingly, physicochemical properties impacting inhalation pharmacokinetics were deemed to be different from those impacting ingestion pharmacokinetics.

Physicochemical properties that showed low or moderate correlation with pharmacokinetic measures were further explored to determine if a combination of properties or non-linear regression could achieve improved predictive power (Figure 1A–C, E–G). The T_{max} regression model (Equation 1) had an $r^2 = 0.84$ (Figure 1D) and utilised the predictors: TPSA ($P = 0.007$), Vol ($P = 0.003$), TPSA*Vol ($P = 0.003$), MW*Vol ($P = 0.005$) and TPSA*MW*Vol ($P = 0.003$). Similarly, the $T_{½}$ regression model (Equation 2) had an $r^2 = 0.87$ (Figure 1H) and utilised the predictors: MW ($P = 0.011$), Vol (P = 0.015), MW^2 ($P = 0.016$), Vol^2 ($P = 0.006$), nrot^2 ($P = 0.028$), MW*Vol ($P = 0.008$) and MW*nrot ($P = 0.032$).

Equation 1: $Ln(Tmax) = 7.62 - 0.1523\ TPSA - 0.0706\ Vol + 0.001010\ TPSA*Vol + 0.0000969\ MW*Vol - 0.00000126\ TPSA*MW*Vol$

Equation 2: $Ln(T_{½}) = -5.44 - 0.1237\ MW + 0.1723\ Vol - 0.000503\ (MW)^2 - 0.001092\ (Vol)^2 + 0.0802\ (nrot)^2 + 0.001519\ MW*Vol - 0.002123$

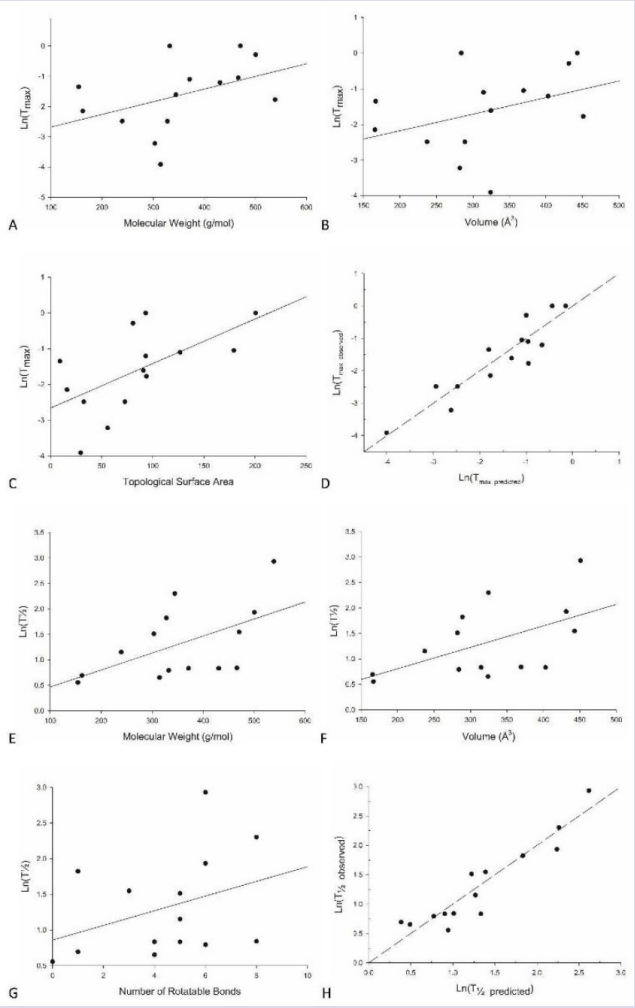

Figure 1: Power of individual and multiple physicochemical parameters for predicting the pharmacokinetic measures T_{max} and $T_{½}$. A) Ln(T_{max}) vs molecular weight. B) Ln(T_{max}) vs molecule volume. C) Ln(T_{max}) vs topological polar surface area. D) Ln(T_{max} observed) vs Ln(T_{max} predicted). E) Ln($T_{½}$) vs molecular weight. F) Ln($T_{½}$) vs molecule volume. G) Ln($T_{½}$) vs number of rotatable bonds. H) Ln(T½ observed) vs Ln($T_{½}$ predicted).

*MW*nrot*

*Equations 1 and 2 describe the natural logarithm (ln) of T_{max} and $T_{½}$, respectively, utilising the terms: topological polar surface area (TPSA), molecular volume (Vol), the product of topological surface area and molecular volume (TPSA*Vol), the product of molecular weight and molecular volume (MW*Vol), the product of topological polar surface area, molecular weight and molecular volume (TPSA*MW*Vol), molecular weight (MW), number of rotatable bonds (nrot), the product of molecular weight and molecular volume (MW*Vol) and the product of molecular weight and number of freely rotatable bonds (MW*nrot).*

Application of the IAP model to predict phytochemical decay in plasma

The IAP model was used to create functional fingerprints predicting compound plasma levels following inhalation (Figure 2A). The functional fingerprints were constructed according to five iterations of the $T_{½}$ function, when plasma levels are said to have reached steady state and 97% of the compound has been cleared from the body.[17] The capacity to predict when a compound achieves steady state is particularly useful for guiding dosage intervals to maintain a threshold PDC for drug efficacy and mitigate the risk of toxicity.[19] The IAP model was applied to two cannabinoids THC and cannabidiol (CBD), to compare predicted T_{max} against *in-vivo* data. The T_{max} for THC and CBD were observed as 0.05 h and 0.11 h, respectively,[40,41] while the predicted T_{max} were 0.02 h and 0.03 h, respectively. Considering that T_{max} predictions within 1.5 h of observation are considered to be accurate predictions,[15] these differences (average 4 min) were considered to be within the acceptable range of pharmacokinetic predictions.

The IAP model was further applied to THC, CBD and the metabolites THC-COOH and 11-OH-THC to compare predicted $T_{½}$ (Figure 2C) against *in-vivo* data (Figure 2B) presented in Nadulski *et al.*[42] Considering that the compounds in Nadulski *et al.*[42] were ingested (not inhaled), only comparisons between their elimination half-lives ($T_{½}$) were made, as $T_{½}$ is only dependent on the compound not its method of intake. For example, the $T_{½}$ for nicotine, taken as either a cigarette, intravenous injection, sucking lozenge, or chewing gum was shown to be in the narrow range of 2.0–2.5 h.[43-45] The $T_{½}$ observed in Nadulski *et al.*[42] for THC-COOH, 11-OH-THC, THC and CBD were 3.93 h, 2.88 h, 1.59 h and 1.56 h, respectively, while the predicted $T_{½}$ were 2.98 h, 2.08 h, 1.63 h and 1.61 h, respectively. The resulting difference between observed and predicted $T_{½}$ across the four compounds was on average 27.7 min. The IAP model was therefore shown to accurately predict both T_{max} and $T_{½}$ and thereby produce functional fingerprints which may be used in pharmacognosy to explore the phytochemistry underpinning the efficacy of medicinal plants.

Case study: Biomatching cannabis phytochemicals to their medicinal effects

The IAP model was applied to explore biomatching between predicted cannabis phytochemical PDC and physiological effects following the smoking of cannabis reported in Greenwald and Stitzer.[38] Predicted plasma THC concentrations aligned closely with reported measures for increases in good mood (Figure 3A). The THC-induced mood-elevating effect following cannabis inhalation is well established and is thought to confer antidepressant-like effects by interacting with the endocannabinoid system.[46,47] Additionally, the predicted lag in plasma THC concentrations (due to the initial inhalation of placebo cigarettes) matched to the observed lag in mood elevation of 0.875 h (Figure 3A). This consistency supports the interpretation of THC as the phytochemical causing mood elevation following cannabis inhalation and highlights the precision and potential applications of the IAP model.

The IAP model was used to explore biomatching between observed antinociceptive effects reported in Greenwald and Stitzer[38] with the combined concentrations of myrcene and caryophyllene (Figure 3B), which have previously shown analgesic and antinociceptive effects in mice.[8,48,49] Predicted plasma levels of myrcene and caryophyllene generally aligned with antinociceptive effects, including alignment of the gradual decrease in antinociceptive effects (0.25–0.85 h, Figure 2B) with the predicted decline in myrcene and caryophyllene plasma concentrations. Whilst Greenwald and Stitzer[38] attribute this observed antinociceptive effect to THC, the onset of antinociception did not align with the inhalation of THC-containing "treatment" cigarettes, but did align with myrcene and caryophyllene which were present in both "treatment" and "placebo" cigarettes. Accordingly, while THC may be contributing via the entourage effect,[8] it appears to be playing a lesser role than myrcene and caryophyllene in antinociception. These results support the ability of the IAP model to accurately predict compound clearance rates after inhalation via predicted $T_{½}$ and highlight how the IAP model may be used to explore phytochemical modes of action by

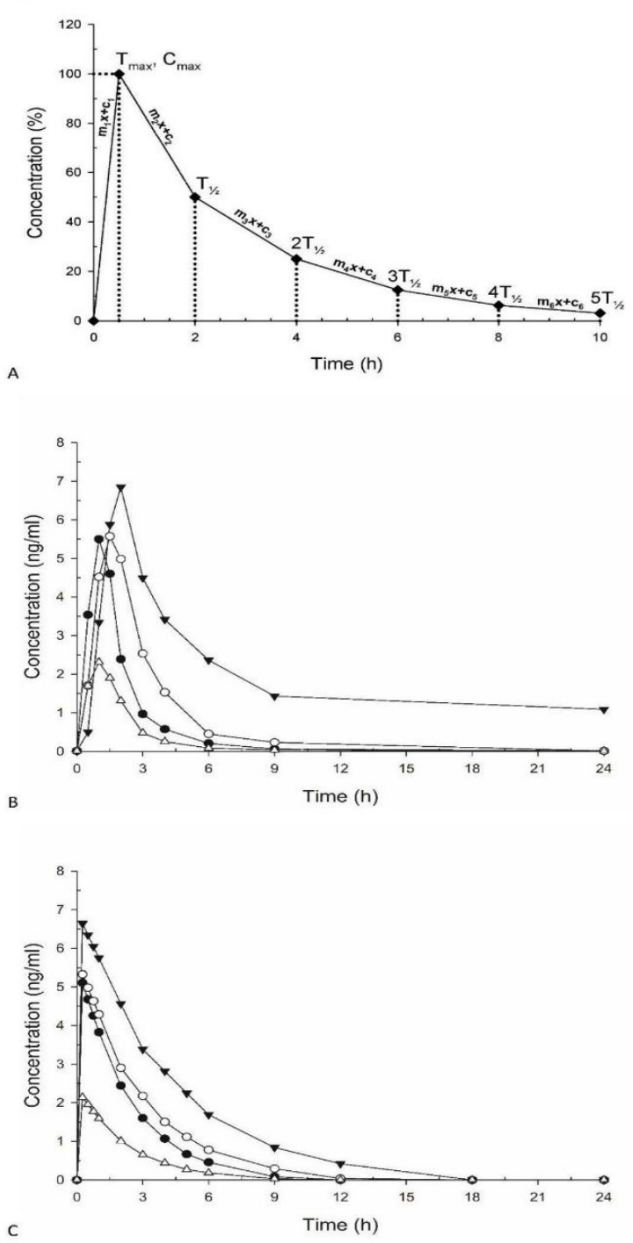

Figure 2: Functional fingerprints for compound plasma levels. A) Schematic representation of the method for constructing functional fingerprints. B) Functional fingerprint of ingested cannabis phytochemicals and associated metabolites, adapted with permission of Wolters Kluwer Health, from Nadulski *et al.* (2005). C) Functional fingerprint of inhaled cannabis phytochemicals and associated metabolites predicted using the IAP model. THC-COOH (▼), THC (●), 11-OH-THC (○) and CBD (△).

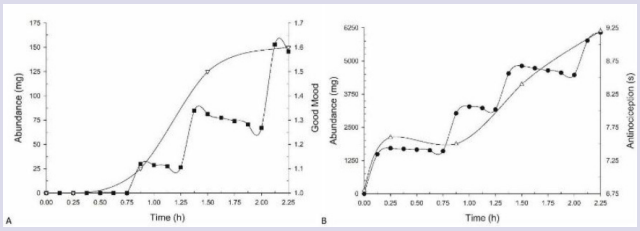

Figure 3: Biomatching of predicted compound plasma levels with observed effects after smoking cannabis and placebo cigarettes. Overlay of plasma concentrations of cannabis phytochemicals predicted using the IAP model, with physiological effects data adapted with permission of Elsevier, from Greenwald and Stitzer (2000). A) THC levels (■) biomatched with patient reported good mood (▽). B) Combined myrcene and caryophyllene levels (●) biomatched with antinociceptive effect (△).

biomatching during pharmacognosy analyses of medicinal plants.

CONCLUSION

The present study describes the inhalation absorption prediction (IAP) model, an *in-silico* pharmacokinetic model for predicting plasma drug concentration (PDC) following inhalation. The model calculates compound accumulation rate via T_{max} and compound clearance rate via $T_{½}$, to achieve a functional fingerprint which accurately predicts temporal changes of PDC. The model demonstrates biomatching between medicinal effects; good mood and antinociception, with predicted plasma levels of THC and combined levels of myrcene and caryophyllene, respectively. The alignment between timings of the observed medicinal effects and increased plasma levels supports the application of the IAP model to explore the modes of action of medicinal phytochemicals and to guide drug loading dosages and frequency to achieve and maintain therapeutic PDC. The IAP model is therefore a novel and powerful tool for guiding future clinical trials of inhaled medicinal compounds.

ACKNOWLEDGEMENT

The authors would like to thank Nutrifield Pty Ltd for supporting this work and providing the required resources.

CONFLICT OF INTEREST

The authors wish to confirm that there are no conflicts of interest associated with this publication.

ABBREVIATIONS

CBD: cannabidiol; **C_{max}:** maximal plasma concentration; **IAP:** Inhalation absorption prediction; **Log P:** Lipophilicity descriptor; **MW:** molecular weight; **Nrot:** Number of rotatable bonds; **PCAP:** phytochemical absorption prediction; **PDC:** plasma drug concentrations; **$T_{½}$:** Time to reach half maximal concentration; **THC:** delta-9-tetrathydrocannabinol; **T_{max}:** Time of maximal concentration; **TPSA:** Topological surface area; **Vol:** molecular volume.

REFERENCES

1. Zuardi AW. History of cannabis as a medicine: a review. Revista Brasileira De Psiquiatría. 2006;28(2):153-7.
2. Bonini SA, Premoli M, Tambaro S, Kumar A, Maccarinelli G, Memo M, *et al. Cannabis sativa:* A comprehensive ethnopharmacological review of a medicinal plant with a long history. Journal of Ethnopharmacology. 2018.
3. Pellati F, Borgonetti V, Brighenti V, Biagi M, Benvenuti S, Corsi L. *Cannabis sativa L. and* Nonpsychoactive Cannabinoids: Their Chemistry and Role against Oxidative Stress, Inflammation and Cancer. Bio Med Research International. 2018;2018:1-15.
4. Elliott J, DeJean D, Clifford T, Coyle D, Potter BK, Skidmore B, *et al.* Cannabis-based products for pediatric epilepsy: a systematic review. Epilepsia. 2019;60(1):6-19.
5. Kalant H. Medicinal use of cannabis: history and current status. Pain Research and Management. 2001;6(2):80-91.
6. Hazekamp A, Ware MA, Muller-Vahl KR, Abrams D, Grotenhermen F. The medicinal use of cannabis and cannabinoids—an international cross-sectional survey on

administration forms. Journal of Psychoactive Drugs. 2013;45(3):199-210.
7. Hazekamp A. Cannabis review: Leiden University: Department of Plant Metobolomics. 2009.
8. Russo EB. Taming THC: potential cannabis synergy and phytocannabinoid-terpenoid entourage effects. British Journal of Pharmacology. 2011;163(7):1344-64.
9. Rasoanaivo P, Wright CW, Willcox ML, Gilbert B. Whole plant extracts versus single compounds for the treatment of malaria: synergy and positive interactions. Malaria Journal. 2011;10(Suppl 1):S4.
10. Sanchez-Ramos J. The entourage effect of the phytocannabinoids. Annals of Neurology. 2015;77(6):1083.
11. DeWaterbeemd VH, Gifford E. ADMET *in silico* modelling: towards prediction paradise?. Nature Reviews Drug Discovery. 2003;2(3):192-204.
12. Selby-Pham SN, Miller RB, Howell K, Dunshea F, Bennett LE. Physicochemical properties of dietary phytochemicals can predict their passive absorption in the human small intestine. Scientific Reports. 2017;7(1):1931.
13. Selby-Pham SNB, Howell KS, Dunshea FR, Ludbey J, Lutz A, Bennett LE. Statistical modelling coupled with LC-MS analysis to predict human upper intestinal absorption of phytochemical mixtures. Food Chemistry. 2018;245:353-63.
14. Selby-Pham SNB. Predictive modelling of upper intestinal absorption of dietary phytochemicals to optimise for health benefits in humans, in Veterinary and Agricultural Sciences. The University of Melbourne. 2017.
15. Wise K, Selby-Pham S, Bennett L, Selby-Pham J. Pharmacokinetic properties of phytochemicals in Hypericum perforatum influence efficacy of regulating oxidative stress. Phytomedicine. 2019;59: 152763.
16. Selby-Pham J, Selby-Pham SN, Wise K, Bennett LE. Understanding health-related properties of bushmint (Hyptis) by pharmacokinetic modelling of intestinal absorption. Phytochemistry Letters. 2018;26:16-9.
17. Visser M. Translating Pharmacokinetic and Pharmacodynamic Data into Practice. Veterinary Clinics of North America: Exotic Animal Practice. 2018;21(2):169-82.
18. Derendorf H, Hochhaus G, Meibohm B, Möllmann H, Barth J. Pharmacokinetics and pharmacodynamics of inhaled corticosteroids. Journal of Allergy and Clinical Immunology. 1998;101(4):S440-6.
19. Garcia-Contreras L, Muttil P, Fallon JK, Kabadi M, Gerety R, Hickey AJ. Pharmacokinetics of sequential doses of capreomycin powder for inhalation in guinea pigs. Antimicrobial Agents Chemotherapy. 2012;56(5):2612-8.
20. Patton JS, Fishburn CS, Weers JG. The lungs as a portal of entry for systemic drug delivery. Proceedings of the American Thoracic Society. 2004;1(4):338-44.
21. Cass LM, Efthymiopoulos C, Bye A. Pharmacokinetics of zanamivir after intravenous, oral, inhaled or intranasal administration to healthy volunteers. Clinical Pharmacokinetics. 1999;36(1):1-11.
22. Cone EJ. Pharmacokinetics and pharmacodynamics of cocaine. Journal of Analytical Toxicology. 1995;19(6):459-78.
23. Drollmann A, Nave R, Steinijans VW, Baumgärtner E, Bethke TD. Equivalent pharmacokinetics of the active metabolite of ciclesonide with and without use of the AeroChamber Plus™ spacer for inhalation. Clinical Pharmacokinetics. 2006;45(7):729-36.
24. Jager W, Našel B, Našel C, Binder R, Stimpfl T, Vycudilik W, *et al.* Pharmacokinetic studies of the fragrance compound 1, 8-cineol in humans during inhalation. Chemical Senses. 1996;21(4):477-80.
25. Kirby S, Falcoz C, Daniel M, Milleri S, Squassante L, Ziviani L, *et al.* Salmeterol and fluticasone propionate given as a combination. European Journal of Clinical Pharmacology. 2001;56(11):781-91.
26. Lecaillon J, Kaiser G, Palmisano M, Morgan J, Della CG. Pharmacokinetics and tolerability of formoterol in healthy volunteers after a single high dose of Foradil dry powder inhalation via Aerolizer TM. European Journal of Clinical Pharmacology. 1999;55(2):131-8.
27. Marsot A, Audebert C, Attolini L, Lacarelle B, Micallef J, Blin O. Comparison of cannabinoid concentrations in plasma, oral fluid and urine in occasional cannabis smokers after smoking cannabis cigarette. Journal of Pharmacy and Pharmaceutical Sciences. 2016;19(3):411-22.
28. Neale M, Brown K, Foulds R, Lal S, Morris D, Thomas D. The pharmacokinetics of nedocromil sodium, a new drug for the treatment of reversible obstructive airways disease, in human volunteers and patients with reversible obstructive airways disease. British Journal of Clinical Pharmacology. 1987;24(4):493-501.
29. Richards R, Fowler C, Simpson S, Renwick AG, Holgate ST. Inhaled histamine increases the rate of absorption of sodium cromoglycate from the lung. British Journal of Clinical Pharmacology. 1992;33(3):337-41.
30. Rix PJ, Vick A, Attkins NJ, Barker GE, Bott AW, Alcorn H, *et al.* Pharmacokinetics, pharmacodynamics, safety and tolerability of nebulized sodium nitrite (AIR001) following repeat-dose inhalation in healthy subjects. Clinical Pharmacokinetics. 2015;54(3):261-72.
31. Schneider NG, Olmstead RE, Franzon MA, Lunell E. The nicotine inhaler. Clinical Pharmacokinetics. 2001;40(9):661-84.
32. Skoner DP. Pharmacokinetics, pharmacodynamics and the delivery of pediatric bronchodilator therapy. Journal of Allergy and Clinical Immunology. 2000;106(3):S158-64.
33. Spyker DA, Munzar P, Cassella JV. Pharmacokinetics of loxapine following inhalation of a thermally generated aerosol in healthy volunteers. The Journal of Clinical Pharmacology. 2010;50(2):169-79.
34. Thorsson L, Edsbacker S, Conradson T. Lung deposition of budesonide from Turbuhaler is twice that from a pressurized metered-dose inhaler P-MDI. European Respiratory Journal. 1994;7(10):1839-44.
35. Usmani OS, Molimard M, Gaur V, Gogtay J, Singh GJ, Malhotra G, *et al.* Scientific rationale for determining the bioequivalence of inhaled drugs. Clinical Pharmacokinetics. 2017;56(10):1139-54.
36. Vaisman N, Koren G, Goldstein D, Canny GJ, Tan Y, Soldin S, *et al.* Pharmacokinetics of inhaled salbutamol in patients with cystic fibrosis versus healthy young adults. The Journal of Pediatrics. 1987;111(6):914-7.
37. Mediavilla V, Steinemann S. Essential oil of *Cannabis sativa* L. strains. Journal of the International Hemp Association. 1997;4:80-2.
38. Greenwald MK, Stitzer ML. Antinociceptive, subjective and behavioral effects of smoked marijuana in humans. Drug and Alcohol Dependence. 2000;59(3):261-75.
39. Hinkle DE, Wiersma W, Jurs SG. Applied statistics for the behavioral sciences. Boston, USA: Houghton Mifflin. 1988.
40. Hollister L, Gillespie H, Ohlsson A, Lindgren JE, Wahlen A, Agurell S. Do Plasma Concentrations of Δ9-Tetrahydrocannabinol Reflect the Degree of Intoxication?. The Journal of Clinical Pharmacology. 1981;21(S1):171S-7S.
41. Newmeyer MN, Swortwood MJ, Barnes AJ, Abulseoud OA, Scheidweiler KB, Huestis MA. Free and glucuronide whole blood cannabinoids' pharmacokinetics after controlled smoked, vaporized and oral cannabis administration in frequent and occasional cannabis users: identification of recent cannabis intake. Clinical Chemistry. 2016;62(11):1579-92.
42. Nadulski T, Pragst F, Weinberg G, Roser P, Schnelle M, Fronk EM, *et al.* Randomized, double-blind, placebo-controlled study about the effects of cannabidiol (CBD) on the pharmacokinetics of Δ^9-tetrahydrocannabinol (THC) after oral application of THC verses standardized cannabis extract. Therapeutic Drug Monitoring. 2005;27(6):799-810.
43. Benowitz NL, Hukkanen J, Jacob P. 3rd, Nicotine chemistry, metabolism, kinetics and biomarkers, in Handbook of experimental pharmacology. Springer: Berlin, Germany. 2009;29-60.
44. Feyerabend C, Ings R, Russel M. Nicotine pharmacokinetics and its application to intake from smoking. British Journal of Clinical Pharmacology. 1985;19(2):239-47.
45. Choi JH, Dresler CM, Norton MR, Strahs KR. Pharmacokinetics of a nicotine polacrilex lozenge. Nicotine and Tobacco Research. 2003;5(5):635-44.
46. El-Alfy AT, Ivey K, Robinson K, Ahmed S, Radwan M, Slade D, *et al.* Antidepressant-like effect of Δ9-tetrahydrocannabinol and other cannabinoids isolated from *Cannabis sativa* L. Pharmacology Biochemistry Behavior. 2010;95(4):434-42.
47. Ashton C, Moore P. Endocannabinoid system dysfunction in mood and related disorders. Acta Psychiatrica Scandinavica. 2011;124(4):250-61.
48. Rao V, Menezes A, Viana G. Effect of myrcene on nociception in mice. Journal of Pharmacy Pharmacology. 1990;42(12):877-8.
49. Katsuyama S, Mizoguchi H, Kuwahata H, Komatsu T, Nagaoka K, Nakamura H, *et al.* Involvement of peripheral cannabinoid and opioid receptors in β-caryophyllene-induced antinociception. European Journal of Pain. 2013;17(5):664-75.

SUMMARY

The Inhalation absorption prediction (IAP) model is a novel *in-silico* strategy for modelling of phytochemical pharmacokinetics post inhalation based on predicted time of maximal absorption (T_{max}) and elimination half-life ($T_{½}$). Application of the IAP model was applied to the *in-silico* pharmacognosy exploration of medicinal cannabis, which identified caryophyllene and myrcene as associated with antinociception and THC as associated with mood elevation.

PICTORIAL ABSTRACT

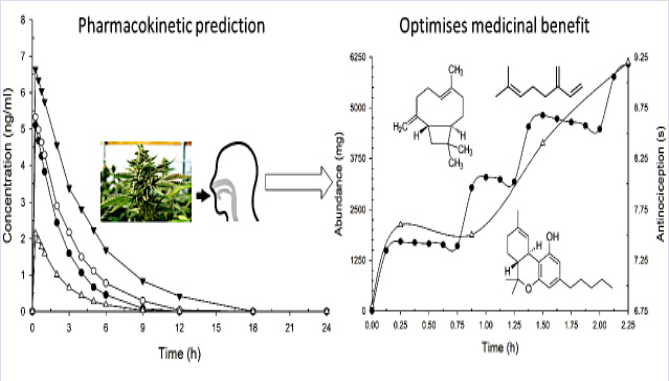

ABOUT AUTHORS

Mr. Kimber Wise, is undertaking his MSc in Food Science at RMIT University. He is also working as a Research and Development Scientist within the Nutrifield R&D team.

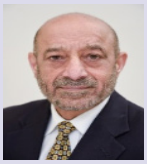

Prof. Harsharn Gill, is the head of the Food Research and Innovation Centre at RMIT University. He has over 25 years' experience in leading and managing food, nutrition and health R&D in private and public sectors.

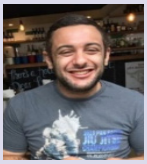

Dr. Jamie Selby-Pham, is the Head of R&D/ Chief Research Scientist within the Nutrifield R&D team. He completed his PhD in Biosciences at the University of Melbourne.

SUPPLEMENTARY TABLE

Table S1: Training data set for inhalation absorption prediction (IAP) model.

Compound	T_{max} (h)	T_{max} Reference	$T_{½}$ (h)	$T_{½}$ Reference
Budesonide	0.3	(Thorsson, Edsbacker *et al.* 1994)	2.3	(Thorsson, Edsbacker *et al.* 1994)
Cocaine	0.04	(Cone 1995)	4.54	(Cone 1995)
THC	0.02	(Marsot, Audebert *et al.* 2016)	1.92	(Marsot, Audebert *et al.* 2016)
Formoterol	0.2	*(Usmani, Molimard et al.* 2017)	10	(Lecaillon, Kaiser *et al.* 1999)
Nedocromil	0.3333	(Neale, Brown *et al.* 1987)	2.3	(Neale, Brown *et al.* 1987)
Nicotine	0.11667	(Schneider, Olmstead *et al.* 2001)	2	(Schneider, Olmstead *et al.* 2001)
Salbutamol	0.08333	(Skoner 2000)	3.16667	(Vaisman, Koren *et al.* 1987)
Fluticasone furoate	0.17	(Rix, Vick *et al.* 2015)	18.75	(Rix, Vick et al. 2015)
Loxapine	0.08317	(Spyker, Munzar *et al.* 2010)	6.19	(Spyker, Munzar *et al.* 2010)
sodium cromoglycate	0.35	(Richards, Fowler *et al.* 1992)	2.31667	(Richards, Fowler *et al.* 1992)
Eucalyptol	0.2595	(Jäger, Našel *et al.* 1996)	1.74333	(Jäger, Našel *et al.* 1996)
Desisobutyryl-ciclesonide	1	(Drollmann, Nave *et al.* 2006)	4.7	(Drollmann, Nave *et al.* 2006)
Zanamivir	1	(Cass, Efthymiopoulos *et al.* 1999)	2.21	(Cass, Efthymiopoulos *et al.* 1999)
fluticasone propionate	0.75	(Kirby, Falcoz *et al.* 2001)	6.91	(Kirby, Falcoz *et al.* 2001)

Table S2: Pearson correlations between physicochemical properties.

Physicochemical properties	Molecular weight	Log P	Total Polar Surface Area	Number of Freely Rotatable Bonds
Log P	$r^2 = 0.0453$			
	$P = 0.465$			
Total Polar Surface Area	$r^2 = 0.279$	$r^2 = 0.4451$		
	$P = 0.052$	$P = 0.009$		
Number of Freely Rotatable Bonds	$r^2 = 0.3382$	$r^2 = 0.0811$	$r^2 = 0.5171$	
	$P = 0.029$	$P = 0.324$	$P = 0.004$	
Volume	$r^2 = 0.9517$	$r^2 = 0.1178$	$r^2 = 0.1734$	$r^2 = 0.2692$
	$P < 0.001$	P = 0.230	$P = 0.139$	$P = 0.057$

Table S3: Linear relationship between physicochemical properties and pharmacokinetic measures.

Pharmacokinetic measure	Molecular weight	Log P	TPSA	Nrot	Volume
T_{max}	$r^2 = 0.1694$	$r^2 = 0.1175$	$r^2 = 0.3321$	$r^2 = 0.0291$	$r^2 = 0.1624$
	$P = 0.144$	$P = 0.230$	$P = 0.031$	$P = 0.560$	$P = 0.153$
$T_{1/2}$	$r^2 = 0.2788$	$r^2 = 0.1220$	$r^2 = 0.0001$	$r^2 = 0.1082$	$r^2 = 0.2563$
	$P = 0.052$	$P = 0.221$	$P = 0.980$	$P = 0.251$	$P = 0.065$